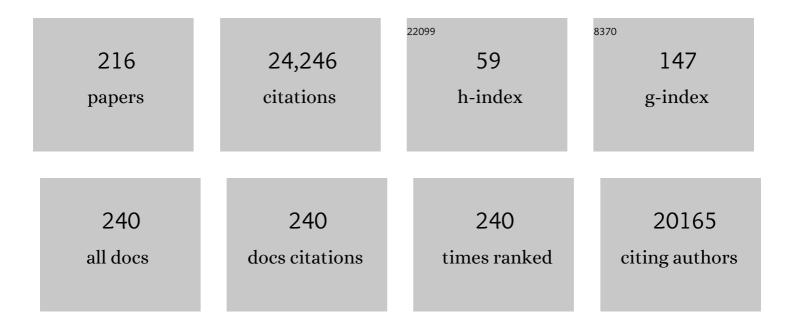
## Dmitri I Svergun

List of Publications by Year in descending order

Source: https://exaly.com/author-pdf/7578606/publications.pdf Version: 2024-02-01



#	Article	IF	CITATIONS
1	<scp>EFAMIX</scp> , a tool to decompose inline chromatography <scp>SAXS</scp> data from partially overlapping components. Protein Science, 2022, 31, 269-282.	3.1	16
2	The prion protein and its ligands: Insights into structure-function relationships. Biochimica Et Biophysica Acta - Molecular Cell Research, 2022, 1869, 119240.	1.9	10
3	Artificial neural networks for solution scattering data analysis. Structure, 2022, 30, 900-908.e2.	1.6	4
4	Lev Feigin (1928–2022). Acta Crystallographica Section A: Foundations and Advances, 2022, 78, .	0.0	0
5	Capturing the Conformational Ensemble of the Mixed Folded Polyglutamine Protein Ataxin-3. Structure, 2021, 29, 70-81.e5.	1.6	8
6	The allosteric modulation of complement C5 by knob domain peptides. ELife, 2021, 10, .	2.8	21
7	Restoring structural parameters of lipid mixtures from small-angle X-ray scattering data. Journal of Applied Crystallography, 2021, 54, 169-179.	1.9	17
8	Self-assembly and regulation of protein cages from pre-organised coiled-coil modules. Nature Communications, 2021, 12, 939.	5.8	28
9	<i>ATSAS 3.0</i> : expanded functionality and new tools for small-angle scattering data analysis. Journal of Applied Crystallography, 2021, 54, 343-355.	1.9	512
10	Limitations of the iterative electron density reconstruction algorithm from solution scattering data. Nature Methods, 2021, 18, 244-245.	9.0	5
11	Comment on the Optimal Parameters to Derive Intrinsically Disordered Protein Conformational Ensembles from Small-Angle X-ray Scattering Data Using the Ensemble Optimization Method. Journal of Chemical Theory and Computation, 2021, 17, 2014-2021.	2.3	13
12	Hallmarks of <i>Alpha-</i> and <i>Betacoronavirus</i> non-structural protein 7+8 complexes. Science Advances, 2021, 7, .	4.7	20
13	Anomalous SAXS at P12 beamline EMBL Hamburg: instrumentation and applications. Journal of Synchrotron Radiation, 2021, 28, 812-823.	1.0	9
14	Molecular basis of F-actin regulation and sarcomere assembly via myotilin. PLoS Biology, 2021, 19, e3001148.	2.6	9
15	Structural analysis of the SRP Alu domain from Plasmodium falciparum reveals a non-canonical open conformation. Communications Biology, 2021, 4, 600.	2.0	5
16	Molecular model of a sensor of two-component signaling system. Scientific Reports, 2021, 11, 10774.	1.6	14
17	Structure of the endocytic adaptor complex reveals the basis for efficient membrane anchoring during clathrin-mediated endocytosis. Nature Communications, 2021, 12, 2889.	5.8	13
18	ASAXS measurements on ferritin and apoferritin at the bioSAXS beamline P12 (PETRA III, DESY). Journal of Applied Crystallography, 2021, 54, 830-838.	1.9	6

#	Article	IF	CITATIONS
19	Order from disorder in the sarcomere: FATZ forms a fuzzy but tight complex and phase-separated condensates with $\hat{l}\pm$ -actinin. Science Advances, 2021, 7, .	4.7	15
20	Autism-associated SHANK3 missense point mutations impact conformational fluctuations and protein turnover at synapses. ELife, 2021, 10, .	2.8	14
21	pUL21 is a viral phosphatase adaptor that promotes herpes simplex virus replication and spread. PLoS Pathogens, 2021, 17, e1009824.	2.1	19
22	Mechanism of activation and regulation of deubiquitinase activity in MINDY1 and MINDY2. Molecular Cell, 2021, 81, 4176-4190.e6.	4.5	18
23	Structure and dynamics of UBA5-UFM1 complex formation showing new insights in the UBA5 activation mechanism. Journal of Structural Biology, 2021, 213, 107796.	1.3	2
24	PED in 2021: a major update of the protein ensemble database for intrinsically disordered proteins. Nucleic Acids Research, 2021, 49, D404-D411.	6.5	95
25	Small-angle X-ray and neutron scattering. Nature Reviews Methods Primers, 2021, 1, .	11.8	77
26	The USR domain of USF1 mediates NF-Y interactions and cooperative DNA binding. International Journal of Biological Macromolecules, 2021, 193, 401-413.	3.6	0
27	The Cytoplasmic Tail of Influenza A Virus Hemagglutinin and Membrane Lipid Composition Change the Mode of M1 Protein Association with the Lipid Bilayer. Membranes, 2021, 11, 772.	1.4	8
28	The Disease Associated Tau35 Fragment has an Increased Propensity to Aggregate Compared to Full-Length Tau. Frontiers in Molecular Biosciences, 2021, 8, 779240.	1.6	8
29	Probing the existence of non-thermal Terahertz radiation induced changes of the protein solution structure. Scientific Reports, 2021, 11, 22311.	1.6	4
30	Ligands binding to the prion protein induce its proteolytic release with therapeutic potential in neurodegenerative proteinopathies. Science Advances, 2021, 7, eabj1826.	4.7	18
31	Clustering in ferronematics—The effect of magnetic collective ordering. IScience, 2021, 24, 103493.	1.9	3
32	Self-assembly and cellular effect of tau35, a disease-associated tau fragment Alzheimer's and Dementia, 2021, 17 Suppl 3, e052072.	0.4	0
33	SASBDB: Towards an automatically curated and validated repository for biological scattering data. Protein Science, 2020, 29, 66-75.	3.1	158
34	Structural Kinetics of MsbA Investigated by Stopped-Flow Time-Resolved Small-Angle X-Ray Scattering. Structure, 2020, 28, 348-354.e3.	1.6	28
35	BILMIX: a new approach to restore the size polydispersity and electron density profiles of lipid bilayers from liposomes using small-angle X-ray scattering data. Journal of Applied Crystallography, 2020, 53, 236-243.	1.9	7
36	Effect of the concentration of protein and nanoparticles on the structure of biohybrid nanocomposites. Biopolymers, 2020, 111, e23342.	1.2	7

#	Article	IF	CITATIONS
37	Structural basis for DNA recognition and allosteric control of the retinoic acid receptors RAR–RXR. Nucleic Acids Research, 2020, 48, 9969-9985.	6.5	17
38	Methods, development and applications of small-angle X-ray scattering to characterize biological macromolecules in solution. Current Research in Structural Biology, 2020, 2, 164-170.	1.1	41
39	The F1 loop of the talin head domain acts as a gatekeeper in integrin activation and clustering. Journal of Cell Science, 2020, 133, .	1.2	18
40	Structure-Based Identification and Functional Characterization of a Lipocalin in the Malaria Parasite Plasmodium falciparum. Cell Reports, 2020, 31, 107817.	2.9	23
41	Molecular mechanism of leukocidin GH–integrin CD11b/CD18 recognition and species specificity. Proceedings of the National Academy of Sciences of the United States of America, 2020, 117, 317-327.	3.3	17
42	The basics of small-angle neutron scattering (SANS for new users of structural biology). EPJ Web of Conferences, 2020, 236, 03001.	0.1	3
43	Anomeric Selectivity of Trehalose Transferase with Rare <scp>l</scp> -Sugars. ACS Catalysis, 2020, 10, 8835-8839.	5.5	1
44	RovC - a novel type of hexameric transcriptional activator promoting type VI secretion gene expression. PLoS Pathogens, 2020, 16, e1008552.	2.1	6
45	Structure of a collagen VI α3 chain VWA domain array: adaptability and functional implications of myopathy causing mutations. Journal of Biological Chemistry, 2020, 295, 12755-12771.	1.6	7
46	Adding Size Exclusion Chromatography (SEC) and Light Scattering (LS) Devices to Obtain High-Quality Small Angle X-Ray Scattering (SAXS) Data. Crystals, 2020, 10, 975.	1.0	48
47	A Giant Extracellular Matrix Binding Protein of <i>Staphylococcus epidermidis</i> Binds Surface-Immobilized Fibronectin via a Novel Mechanism. MBio, 2020, 11, .	1.8	9
48	Selection, biophysical and structural analysis of synthetic nanobodies that effectively neutralize SARS-CoV-2. Nature Communications, 2020, 11, 5588.	5.8	132
49	An automated data processing and analysis pipeline for transmembrane proteins in detergent solutions. Scientific Reports, 2020, 10, 8081.	1.6	12
50	Btk SH2-kinase interface is critical for allosteric kinase activation and its targeting inhibits B-cell neoplasms. Nature Communications, 2020, 11, 2319.	5.8	23
51	Molecular Mechanisms of the Interactions of N-(2-Hydroxypropyl)methacrylamide Copolymers Designed for Cancer Therapy with Blood Plasma Proteins. Pharmaceutics, 2020, 12, 106.	2.0	12
52	Structural Modeling Using Solution Small-Angle X-ray Scattering (SAXS). Journal of Molecular Biology, 2020, 432, 3078-3092.	2.0	61
53	Tetrameric Structures of Inorganic CBS-Pyrophosphatases from Various Bacterial Species Revealed by Small-Angle X-ray Scattering in Solution. Biomolecules, 2020, 10, 564.	1.8	4
54	Structural Analyses of Intrinsically Disordered Proteins by Small-Angle X-Ray Scattering. Methods in Molecular Biology, 2020, 2141, 249-269.	0.4	8

#	Article	IF	CITATIONS
55	A beginner's guide to solution small-angle X-ray scattering (SAXS). Biochemist, 2020, 42, 36-42.	0.2	4
56	Simulation of small-angle X-ray scattering data of biological macromolecules in solution. Journal of Applied Crystallography, 2020, 53, 536-539.	1.9	7
57	Rapid screening of <i>in cellulo</i> grown protein crystals via a small-angle X-ray scattering/X-ray powder diffraction synergistic approach. Journal of Applied Crystallography, 2020, 53, 1169-1180.	1.9	17
58	Software Tools for Biological Structural Analysis Using Small-Angle X-Ray Solution Scattering. , 2020, , 1-7.		0
59	The quaternary structure of insulin glargine and glulisine under formulation conditions. Biophysical Chemistry, 2019, 253, 106226.	1.5	9
60	Molecular Organization of Soluble Type III Secretion System Sorting Platform Complexes. Journal of Molecular Biology, 2019, 431, 3787-3803.	2.0	28
61	Studying Conformational Changes of the Yersinia Type-III-Secretion Effector YopO in Solution by Integrative Structural Biology. Structure, 2019, 27, 1416-1426.e3.	1.6	19
62	Solution structure and flexibility of the condensin HEAT-repeat subunit Ycg1. Journal of Biological Chemistry, 2019, 294, 13822-13829.	1.6	9
63	The dimeric ectodomain of the alkali-sensing insulin receptor–related receptor (ectoIRR) has a droplike shape. Journal of Biological Chemistry, 2019, 294, 17790-17798.	1.6	10
64	The free energy landscape of the oncogene protein E7 of human papillomavirus type 16 reveals a complex interplay between ordered and disordered regions. Scientific Reports, 2019, 9, 5822.	1.6	8
65	Structure of ATP citrate lyase and the origin of citrate synthase in the Krebs cycle. Nature, 2019, 568, 571-575.	13.7	101
66	Octa-repeat domain of the mammalian prion protein mRNA forms stable A-helical hairpin structure rather than G-quadruplexes. Scientific Reports, 2019, 9, 2465.	1.6	3
67	An NAD+ Phosphorylase Toxin Triggers Mycobacterium tuberculosis Cell Death. Molecular Cell, 2019, 73, 1282-1291.e8.	4.5	58
68	Shedding Light on the Interaction of Human Anti-Apoptotic Bcl-2 Protein with Ligands through Biophysical and in Silico Studies. International Journal of Molecular Sciences, 2019, 20, 860.	1.8	25
69	Structural properties of [2Fe-2S] ISCA2-IBA57: a complex of the mitochondrial iron-sulfur cluster assembly machinery. Scientific Reports, 2019, 9, 18986.	1.6	22
70	Human MICAL1: Activation by the small GTPase Rab8 and smallâ€angle Xâ€ray scattering studies on the oligomerization state of MICAL1 and its complex with Rab8. Protein Science, 2019, 28, 150-166.	3.1	7
71	Conformational characterization of full-length X-chromosome-linked inhibitor of apoptosis protein (XIAP) through an integrated approach. IUCrJ, 2019, 6, 948-957.	1.0	5
72	Functional interaction of low-homology FRPs from different cyanobacteria with Synechocystis OCP. Biochimica Et Biophysica Acta - Bioenergetics, 2018, 1859, 382-393.	0.5	13

#	Article	IF	CITATIONS
73	Disease Variants of FGFR3 Reveal Molecular Basis for the Recognition and Additional Roles for Cdc37 in Hsp90 Chaperone System. Structure, 2018, 26, 446-458.e8.	1.6	13
74	Epsin and Sla2 form assemblies through phospholipid interfaces. Nature Communications, 2018, 9, 328.	5.8	47
75	Saposin Lipid Nanoparticles: A Highly Versatile and Modular Tool for Membrane Protein Research. Structure, 2018, 26, 345-355.e5.	1.6	69
76	Macromolecular <i>p</i> HPMA-Based Nanoparticles with Cholesterol for Solid Tumor Targeting: Behavior in HSA Protein Environment. Biomacromolecules, 2018, 19, 470-480.	2.6	17
77	CHROMIXS: automatic and interactive analysis of chromatography-coupled small-angle X-ray scattering data. Bioinformatics, 2018, 34, 1944-1946.	1.8	219
78	Signaling ammonium across membranes through an ammonium sensor histidine kinase. Nature Communications, 2018, 9, 164.	5.8	36
79	Prp19/Pso4 Is an Autoinhibited Ubiquitin Ligase Activated by Stepwise Assembly of Three Splicing Factors. Molecular Cell, 2018, 69, 979-992.e6.	4.5	28
80	Structural model of human dUTPase in complex with a novel proteinaceous inhibitor. Scientific Reports, 2018, 8, 4326.	1.6	15
81	Optical and Structural Characterization of a Chronic Myeloid Leukemia DNA Biosensor. ACS Chemical Biology, 2018, 13, 1235-1242.	1.6	3
82	Structural insights of Rm Xyn10A – A prebiotic-producing GH10 xylanase with a non-conserved aglycone binding region. Biochimica Et Biophysica Acta - Proteins and Proteomics, 2018, 1866, 292-306.	1.1	14
83	Structural basis for activation of plasma-membrane Ca2+-ATPase by calmodulin. Communications Biology, 2018, 1, 206.	2.0	30
84	β2-Type Amyloidlike Fibrils of Poly-l-glutamic Acid Convert into Long, Highly Ordered Helices upon Dissolution in Dimethyl Sulfoxide. Journal of Physical Chemistry B, 2018, 122, 11895-11905.	1.2	7
85	Recent developments in small-angle X-ray scattering and hybrid method approaches for biomacromolecular solutions. Emerging Topics in Life Sciences, 2018, 2, 69-79.	1.1	29
86	Probing the Architecture of a Multi-PDZ Domain Protein: Structure of PDZK1 in Solution. Structure, 2018, 26, 1522-1533.e5.	1.6	10
87	Comment on "Innovative scattering analysis shows that hydrophobic disordered proteins are expanded in water― Science, 2018, 361, .	6.0	27
88	Structure-specific recognition protein-1 (SSRP1) is an elongated homodimer that binds histones. Journal of Biological Chemistry, 2018, 293, 10071-10083.	1.6	9
89	Multi-channel <i>in situ</i> dynamic light scattering instrumentation enhancing biological small-angle X-ray scattering experiments at the PETRA III beamline P12. Journal of Synchrotron Radiation, 2018, 25, 361-372.	1.0	15
90	Conformational States of ABC Transporter MsbA in a Lipid Environment Investigated by Small-Angle Scattering Using Stealth Carrier Nanodiscs. Structure, 2018, 26, 1072-1079.e4.	1.6	58

#	Article	IF	CITATIONS
91	Structural complexity of the co-chaperone SGTA: a conserved C-terminal region is implicated in dimerization and substrate quality control. BMC Biology, 2018, 16, 76.	1.7	11
92	Quantitative 3D determination of self-assembled structures on nanoparticles using small angle neutron scattering. Nature Communications, 2018, 9, 1343.	5.8	54
93	Consensus Bayesian assessment of protein molecular mass from solution X-ray scattering data. Scientific Reports, 2018, 8, 7204.	1.6	154
94	Integrated beamline control and data acquisition for small-angle X-ray scattering at the P12 BioSAXS beamline at PETRAIII storage ring DESY. Journal of Synchrotron Radiation, 2018, 25, 906-914.	1.0	30
95	Machine Learning Methods for X-Ray Scattering Data Analysis from Biomacromolecular Solutions. Biophysical Journal, 2018, 114, 2485-2492.	0.2	71
96	Direct shape determination of intermediates in evolving macromolecular solutions from small-angle scattering data. IUCrJ, 2018, 5, 402-409.	1.0	20
97	Utilization of Staphylococcal Immune Evasion Protein Sbi as a Novel Vaccine Adjuvant. Frontiers in Immunology, 2018, 9, 3139.	2.2	13
98	Smaller capillaries improve the small-angle X-ray scattering signal and sample consumption for biomacromolecular solutions. Journal of Synchrotron Radiation, 2018, 25, 1113-1122.	1.0	27
99	Analysis of self-assembly of S-layer protein slp-B53 from Lysinibacillus sphaericus. European Biophysics Journal, 2017, 46, 77-89.	1.2	19
100	Structural basis of the interaction between the putative adhesion-involved and iron-regulated FrpD and FrpC proteins of Neisseria meningitidis. Scientific Reports, 2017, 7, 40408.	1.6	10
101	Structure of the mycobacterial ESX-5 type VII secretion system membrane complex by single-particle analysis. Nature Microbiology, 2017, 2, 17047.	5.9	102
102	Combining NMR and small angle X-ray scattering for the study of biomolecular structure and dynamics. Archives of Biochemistry and Biophysics, 2017, 628, 33-41.	1.4	46
103	The Shigella Virulence Factor IcsA Relieves N-WASP Autoinhibition by Displacing the Verprolin Homology/Cofilin/Acidic (VCA) Domain. Journal of Biological Chemistry, 2017, 292, 134-145.	1.6	16
104	A Spring-Loaded Mechanism Governs the Clamp-like Dynamics of the Skp Chaperone. Structure, 2017, 25, 1079-1088.e3.	1.6	34
105	Decoupling of size and shape fluctuations in heteropolymeric sequences reconciles discrepancies in SAXS vs. FRET measurements. Proceedings of the National Academy of Sciences of the United States of America, 2017, 114, E6342-E6351.	3.3	195
106	Highly selective tungstate transporter protein TupA from Desulfovibrio alaskensis G20. Scientific Reports, 2017, 7, 5798.	1.6	10
107	Influenza virus Matrix Protein M1 preserves its conformation with pH, changing multimerization state at the priming stage due to electrostatics. Scientific Reports, 2017, 7, 16793.	1.6	25
108	Progress in small-angle scattering from biological solutions at high-brilliance synchrotrons. IUCrJ, 2017, 4, 518-528.	1.0	67

#	Article	lF	CITATIONS
109	2017 publication guidelines for structural modelling of small-angle scattering data from biomolecules in solution: an update. Acta Crystallographica Section D: Structural Biology, 2017, 73, 710-728.	1.1	205
110	The Molecular Bases of the Dual Regulation of Bacterial Iron Sulfur Cluster Biogenesis by CyaY and IscX. Frontiers in Molecular Biosciences, 2017, 4, 97.	1.6	25
111	Structural reorganization of the chromatin remodeling enzyme Chd1 upon engagement with nucleosomes. ELife, 2017, 6, .	2.8	51
112	Rapid automated superposition of shapes and macromolecular models using spherical harmonics. Journal of Applied Crystallography, 2016, 49, 953-960.	1.9	37
113	Conformational plasticity of RepB, the replication initiator protein of promiscuous streptococcal plasmid pMV158. Scientific Reports, 2016, 6, 20915.	1.6	11
114	Resolution of <i>ab initio</i> shapes determined from small-angle scattering. IUCrJ, 2016, 3, 440-447.	1.0	88
115	Characterization of mAb dimers reveals predominant dimer forms common in therapeutic mAbs. MAbs, 2016, 8, 928-940.	2.6	42
116	Calcium-Driven Folding of RTX Domain β-Rolls Ratchets Translocation of RTX Proteins through Type I Secretion Ducts. Molecular Cell, 2016, 62, 47-62.	4.5	110
117	DARA: a web server for rapid search of structural neighbours using solution small angle X-ray scattering data. Bioinformatics, 2016, 32, 616-618.	1.8	17
118	Dual Role of the Active Site Residues of <i>Thermus thermophilus</i> 3-Isopropylmalate Dehydrogenase: Chemical Catalysis and Domain Closure. Biochemistry, 2016, 55, 560-574.	1.2	2
119	Proteins involved in sleep homeostasis: Biophysical characterization of INC and its partners. Biochimie, 2016, 131, 106-114.	1.3	6
120	Preparing monodisperse macromolecular samples for successful biological small-angle X-ray and neutron-scattering experiments. Nature Protocols, 2016, 11, 2122-2153.	5.5	142
121	The flexibility of a homeodomain transcription factor heterodimer and its allosteric regulation by <scp>DNA</scp> binding. FEBS Journal, 2016, 283, 3134-3154.	2.2	9
122	Structure and target interaction of a G-quadruplex RNA-aptamer. RNA Biology, 2016, 13, 973-987.	1.5	20
123	Potent and selective bivalent inhibitors of BET bromodomains. Nature Chemical Biology, 2016, 12, 1097-1104.	3.9	109
124	Extension of the sasCIF format and its applications for data processing and deposition. Journal of Applied Crystallography, 2016, 49, 302-310.	1.9	18
125	Structural Insights into the Polyphyletic Origins of Glycyl tRNA Synthetases. Journal of Biological Chemistry, 2016, 291, 14430-14446.	1.6	16
126	Death-Associated Protein Kinase Activity Is Regulated by Coupled Calcium/Calmodulin Binding to Two Distinct Sites. Structure, 2016, 24, 851-861.	1.6	21

#	Article	IF	CITATIONS
127	Crystal Structure of the CTP1L Endolysin Reveals How Its Activity Is Regulated by a Secondary Translation Product. Journal of Biological Chemistry, 2016, 291, 4882-4893.	1.6	36
128	SASpy: a PyMOL plugin for manipulation and refinement of hybrid models against small angle X-ray scattering data. Bioinformatics, 2016, 32, 2062-2064.	1.8	30
129	LabDisk for SAXS: a centrifugal microfluidic sample preparation platform for small-angle X-ray scattering. Lab on A Chip, 2016, 16, 1161-1170.	3.1	44
130	Solution Behavior of the Intrinsically Disordered N-Terminal Domain of Retinoid X Receptor $\hat{I}_{\pm}$ in the Context of the Full-Length Protein. Biochemistry, 2016, 55, 1741-1748.	1.2	19
131	Deciphering conformational transitions of proteins by small angle X-ray scattering and normal mode analysis. Physical Chemistry Chemical Physics, 2016, 18, 5707-5719.	1.3	161
132	Maturation of 6S regulatory <scp>RNA</scp> to a highly elongated structure. FEBS Journal, 2015, 282, 4548-4564.	2.2	4
133	<i>A posteriori</i> determination of the useful data range for small-angle scattering experiments on dilute monodisperse systems. IUCrJ, 2015, 2, 352-360.	1.0	78
134	SASBDB, a repository for biological small-angle scattering data. Nucleic Acids Research, 2015, 43, D357-D363.	6.5	279
135	The Redox State Regulates the Conformation of Rv2466c to Activate the Antitubercular Prodrug TP053. Journal of Biological Chemistry, 2015, 290, 31077-31089.	1.6	17
136	Advanced ensemble modelling of flexible macromolecules using X-ray solution scattering. IUCrJ, 2015, 2, 207-217.	1.0	516
137	KSHV but not MHV-68 LANA induces a strong bend upon binding to terminal repeat viral DNA. Nucleic Acids Research, 2015, 43, gkv987.	6.5	15
138	Molecular Basis of Histone Tail Recognition by Human TIP5 PHD Finger and Bromodomain of the Chromatin Remodeling Complex NoRC. Structure, 2015, 23, 80-92.	1.6	59
139	The Conundrum of the High-Affinity NGF Binding Site Formation Unveiled?. Biophysical Journal, 2015, 108, 687-697.	0.2	20
140	Glutamate 270 plays an essential role in K <sup>+</sup> â€activation and domain closure of <i>Thermus thermophilus</i> isopropylmalate dehydrogenase. FEBS Letters, 2015, 589, 240-245.	1.3	5
141	BioSAXS Sample Changer: a robotic sample changer for rapid and reliable high-throughput X-ray solution scattering experiments. Acta Crystallographica Section D: Biological Crystallography, 2015, 71, 67-75.	2.5	181
142	Limiting radiation damage for high-brilliance biological solution scattering: practical experience at the EMBL P12 beamline PETRAIII. Journal of Synchrotron Radiation, 2015, 22, 273-279.	1.0	112
143	Automated Pipeline for Purification, Biophysical and X-Ray Analysis of Biomacromolecular Solutions. Scientific Reports, 2015, 5, 10734.	1.6	99
144	Molecular mechanism for the action of the anti-CD44 monoclonal antibody MEM-85. Journal of Structural Biology, 2015, 191, 214-223.	1.3	13

#	Article	IF	CITATIONS
145	Outcome of the First wwPDB Hybrid/Integrative Methods Task Force Workshop. Structure, 2015, 23, 1156-1167.	1.6	159
146	ISPyB for BioSAXS, the gateway to user autonomy in solution scattering experiments. Acta Crystallographica Section D: Biological Crystallography, 2015, 71, 76-85.	2.5	56
147	A small and robust active beamstop for scattering experiments on high-brilliance undulator beamlines. Journal of Synchrotron Radiation, 2015, 22, 461-464.	1.0	13
148	pyDockSAXS: protein–protein complex structure by SAXS and computational docking. Nucleic Acids Research, 2015, 43, W356-W361.	6.5	61
149	Versatile sample environments and automation for biological solution X-ray scattering experiments at the P12 beamline (PETRA III, DESY). Journal of Applied Crystallography, 2015, 48, 431-443.	1.9	508
150	Correlation Map, a goodness-of-fit test for one-dimensional X-ray scattering spectra. Nature Methods, 2015, 12, 419-422.	9.0	195
151	Ambiguity assessment of small-angle scattering curves from monodisperse systems. Acta Crystallographica Section D: Biological Crystallography, 2015, 71, 1051-1058.	2.5	118
152	The architecture of amyloid-like peptide fibrils revealed by X-ray scattering, diffraction and electron microscopy. Acta Crystallographica Section D: Biological Crystallography, 2015, 71, 882-895.	2.5	50
153	Structural Basis for Antigen Recognition by Transglutaminase 2-specific Autoantibodies in Celiac Disease. Journal of Biological Chemistry, 2015, 290, 21365-21375.	1.6	27
154	RAID3 - An interleukin-6 receptor-binding aptamer with post-selective modification-resistant affinity. RNA Biology, 2015, 12, 1043-1053.	1.5	23
155	Cooperative folding of intrinsically disordered domains drives assembly of a strong elongated protein. Nature Communications, 2015, 6, 7271.	5.8	52
156	Application of SAXS for the Structural Characterization of IDPs. Advances in Experimental Medicine and Biology, 2015, 870, 261-289.	0.8	33
157	A practical guide to small angle Xâ€ray scattering (SAXS) of flexible and intrinsically disordered proteins. FEBS Letters, 2015, 589, 2570-2577.	1.3	461
158	A coiled-coil domain acts as a molecular ruler to regulate O-antigen chain length in lipopolysaccharide. Nature Structural and Molecular Biology, 2015, 22, 50-56.	3.6	55
159	Flexibility of the Linker between the Domains of DNA Methyltransferase SsoII Revealed by Small-Angle X-Ray Scattering: Implications for Transcription Regulation in SsoII Restriction–Modification System. PLoS ONE, 2014, 9, e93453.	1.1	7
160	The C-Terminal Random Coil Region Tunes the Ca2+-Binding Affinity of S100A4 through Conformational Activation. PLoS ONE, 2014, 9, e97654.	1.1	11
161	pE-DB: a database of structural ensembles of intrinsically disordered and of unfolded proteins. Nucleic Acids Research, 2014, 42, D326-D335.	6.5	195
162	Crystal structures of substrate-bound chitinase from the psychrophilic bacterium <i>Moritella marina</i> and its structure in solution. Acta Crystallographica Section D: Biological Crystallography, 2014, 70, 676-684.	2.5	13

#	Article	IF	CITATIONS
163	The CD27L and CTP1L Endolysins Targeting Clostridia Contain a Built-in Trigger and Release Factor. PLoS Pathogens, 2014, 10, e1004228.	2.1	37
164	The Structure and Regulation of Human Muscle α-Actinin. Cell, 2014, 159, 1447-1460.	13.5	178
165	A conformational switch in collybistin determines the differentiation of inhibitory postsynapses. EMBO Journal, 2014, 33, 2113-2133.	3.5	75
166	The histone chaperones Vps75 and Nap1 form ring-like, tetrameric structures in solution. Nucleic Acids Research, 2014, 42, 6038-6051.	6.5	37
167	Interactions of ataxin-3 with its molecular partners in the protein machinery that sorts protein aggregates to the aggresome. International Journal of Biochemistry and Cell Biology, 2014, 51, 58-64.	1.2	18
168	Weak protein–ligand interactions studied by smallâ€angle <scp>X</scp> â€ray scattering. FEBS Journal, 2014, 281, 1974-1987.	2.2	35
169	The SH2 domain of Abl kinases regulates kinase autophosphorylation by controlling activation loop accessibility. Nature Communications, 2014, 5, 5470.	5.8	36
170	Scanning tunneling microscopy and small angle neutron scattering study of mixed monolayer protected gold nanoparticles in organic solvents. Chemical Science, 2014, 5, 1232.	3.7	36
171	Structure of the C.Âelegans ZYG-1 Cryptic Polo Box Suggests a Conserved Mechanism for Centriolar Docking of Plk4 Kinases. Structure, 2014, 22, 1090-1104.	1.6	45
172	Novel thermosensitive telechelic PEGs with antioxidant activity: synthesis, molecular properties and conformational behaviour. RSC Advances, 2014, 4, 41763-41771.	1.7	17
173	Designing a Multimer Allergen for Diagnosis and Immunotherapy of Dog Allergic Patients. PLoS ONE, 2014, 9, e111041.	1.1	20
174	The SH2 Domain of BCR-ABL1 Regulates Kinase Autophosphorylation By Controlling Activation Loop Accessibility. Blood, 2014, 124, 2209-2209.	0.6	0
175	Impact and progress in small and wide angle X-ray scattering (SAXS and WAXS). Current Opinion in Structural Biology, 2013, 23, 748-754.	2.6	160
176	Reconstruction of Quaternary Structure from X-ray Scattering by Equilibrium Mixtures of Biological Macromolecules. Biochemistry, 2013, 52, 6844-6855.	1.2	24
177	Self-Assembly and Conformational Heterogeneity of the AXH Domain ofÂAtaxin-1: An Unusual Example of a Chameleon Fold. Biophysical Journal, 2013, 104, 1304-1313.	0.2	19
178	Report of the wwPDB Small-Angle Scattering Task Force: Data Requirements for Biomolecular Modeling and the PDB. Structure, 2013, 21, 875-881.	1.6	77
179	Applications of small-angle X-ray scattering to biomacromolecular solutions. International Journal of Biochemistry and Cell Biology, 2013, 45, 429-437.	1.2	94
180	A structural model of PpoA derived from SAXS-analysis—Implications for substrate conversion. Biochimica Et Biophysica Acta - Molecular and Cell Biology of Lipids, 2013, 1831, 1449-1457.	1.2	9

#	Article	IF	CITATIONS
181	Nonstructural Proteins 7 and 8 of Feline Coronavirus Form a 2:1 Heterotrimer That Exhibits Primer-Independent RNA Polymerase Activity. Journal of Virology, 2012, 86, 4444-4454.	1.5	73
182	WeNMR: Structural Biology on the Grid. Journal of Grid Computing, 2012, 10, 743-767.	2.5	170
183	Automated acquisition and analysis of small angle X-ray scattering data. Nuclear Instruments and Methods in Physics Research, Section A: Accelerators, Spectrometers, Detectors and Associated Equipment, 2012, 689, 52-59.	0.7	272
184	New developments in the <i>ATSAS</i> program package for small-angle scattering data analysis. Journal of Applied Crystallography, 2012, 45, 342-350.	1.9	1,551
185	Instrumental setup for high-throughput small- and wide-angle solution scattering at the X33 beamline of EMBL Hamburg. Journal of Applied Crystallography, 2012, 45, 489-495.	1.9	65
186	Publication guidelines for structural modelling of small-angle scattering data from biomolecules in solution. Acta Crystallographica Section D: Biological Crystallography, 2012, 68, 620-626.	2.5	125
187	Structure of the Lassa Virus Nucleoprotein Revealed by X-ray Crystallography, Small-angle X-ray Scattering, and Electron Microscopy. Journal of Biological Chemistry, 2011, 286, 38748-38756.	1.6	47
188	Low-resolution structure of a vesicle disrupting α-synuclein oligomer that accumulates during fibrillation. Proceedings of the National Academy of Sciences of the United States of America, 2011, 108, 3246-3251.	3.3	222
189	Structural characterization of proteins and complexes using small-angle X-ray solution scattering. Journal of Structural Biology, 2010, 172, 128-141.	1.3	470
190	The Switch that Does Not Flip: The Blue-Light Receptor YtvA from Bacillus subtilis Adopts an Elongated Dimer Conformation Independent of the Activation State as Revealed by a Combined AUC and SAXS Study. Journal of Molecular Biology, 2010, 403, 78-87.	2.0	35
191	<i>DAMMIF</i> , a program for rapid <i>ab-initio</i> shape determination in small-angle scattering. Journal of Applied Crystallography, 2009, 42, 342-346.	1.9	1,431
192	Low-Resolution Structures of Transient Proteinâ^'Protein Complexes Using Small-Angle X-ray Scattering. Journal of the American Chemical Society, 2009, 131, 4378-4386.	6.6	59
193	Solution Structure of Poly(ethylene) Glycol-Conjugated Hemoglobin Revealed by Small-Angle X-Ray Scattering: Implications for a New Oxygen Therapeutic. Biophysical Journal, 2008, 94, 173-181.	0.2	80
194	Structural Characterization of the Active and Inactive States of Src Kinase in Solution by Small-Angle X-ray Scattering. Journal of Molecular Biology, 2008, 376, 492-505.	2.0	49
195	Dynamics in a Pure Encounter Complex of Two Proteins Studied by Solution Scattering and Paramagnetic NMR Spectroscopy. Journal of the American Chemical Society, 2008, 130, 6395-6403.	6.6	96
196	A Helical Structural Nucleus Is the Primary Elongating Unit of Insulin Amyloid Fibrils. PLoS Biology, 2007, 5, e134.	2.6	229
197	Structural Characterization of Flexible Proteins Using Small-Angle X-ray Scattering. Journal of the American Chemical Society, 2007, 129, 5656-5664.	6.6	1,080
198	Accuracy of molecular mass determination of proteins in solution by small-angle X-ray scattering. Journal of Applied Crystallography, 2007, 40, s245-s249.	1.9	328

#	Article	IF	CITATIONS
199	ATSAS 2.1 – towards automated and web-supported small-angle scattering data analysis. Journal of Applied Crystallography, 2007, 40, s223-s228.	1.9	404
200	Multiple Assembly States of Lumazine Synthase: A Model Relating Catalytic Function and Molecular Assembly. Journal of Molecular Biology, 2006, 362, 753-770.	2.0	43
201	ATSAS2.1, a program package for small-angle scattering data analysis. Journal of Applied Crystallography, 2006, 39, 277-286.	1.9	557
202	Structural and Mutational Analysis of Substrate Complexation by Anthranilate Phosphoribosyltransferase from Sulfolobus solfataricus. Journal of Biological Chemistry, 2006, 281, 21410-21421.	1.6	23
203	Global Rigid Body Modeling of Macromolecular Complexes against Small-Angle Scattering Data. Biophysical Journal, 2005, 89, 1237-1250.	0.2	846
204	Conformational Variability of Nucleo-cytoplasmic Transport Factors. Journal of Biological Chemistry, 2004, 279, 2176-2181.	1.6	74
205	Uniqueness ofab initioshape determination in small-angle scattering. Journal of Applied Crystallography, 2003, 36, 860-864.	1.9	1,759
206	PRIMUS: a Windows PC-based system for small-angle scattering data analysis. Journal of Applied Crystallography, 2003, 36, 1277-1282.	1.9	2,672
207	Conformation of full-length Bruton tyrosine kinase (Btk) from synchrotron X-ray solution scattering. EMBO Journal, 2003, 22, 4616-4624.	3.5	69
208	Small-angle scattering: a view on the properties, structures and structural changes of biological macromolecules in solution. Quarterly Reviews of Biophysics, 2003, 36, 147-227.	2.4	476
209	Determination of Domain Structure of Proteins from X-Ray Solution Scattering. Biophysical Journal, 2001, 80, 2946-2953.	0.2	1,309
210	A Map of Protein-rRNA Distribution in the 70 SEscherichia coli Ribosome. Journal of Biological Chemistry, 2000, 275, 14432-14439.	1.6	92
211	Studies on the conformational changes in the bacterial cell wall biosynthetic enzyme UDP-N-acetylglucosamine enolpyruvyltransferase (MurA). FEBS Journal, 1998, 253, 406-412.	0.2	50
212	Escherichia coliSecA shape and dimensions. FEBS Letters, 1998, 436, 277-282.	1.3	46
213	82 Structural characterization of recombinant catalase-peroxidase from <i>Mycobacterium tuberculosis</i> . Biochemical Society Transactions, 1997, 25, S617-S617.	1.6	4
214	Large differences are observed between the crystal and solution quaternary structures of allosteric aspartate transcarbamylase in the R state. Proteins: Structure, Function and Bioinformatics, 1997, 27, 110-117.	1.5	76
215	Large differences are observed between the crystal and solution quaternary structures of allosteric aspartate transcarbamylase in the R state. , 1997, 27, 110.		1
216	Small-angle X-ray solution scattering study on the dimerization of the FKBP25mem fromLegionella pneumophila. FEBS Letters, 1995, 372, 169-172.	1.3	17